Manuscript submitted to
AIMS' Journals
Volume **X**, Number **0X**, XX **200X**

doi:10.3934/xx.xx.xx.xx

pp. **X–XX**

DYNAMICS OF A METAPOPULATION EPIDEMIC MODEL WITH LOCALIZED CULLING

Luca Bolzoni

Risk Analysis and Genomic Epidemiology Unit
Istituto Zooprofilattico Sperimentale della Lombardia e dell'Emilia Romagna, Via dei Mercati 13
43126 Parma, Italy

Rossella Della Marca and Maria Groppi*

Department of Mathematical, Physical and Computer Sciences
Università di Parma, Parco Area delle Scienze 53/A
43124 Parma, Italy

Alessandra Gragnani

Department of Electronics, Information and Bioengineering (DEIB)
Politecnico di Milano, Piazza Leonardo da Vinci 32
20133 Milan, Italy

(Communicated by the associate editor name)

Abstract. A two–patches metapopulation mathematical model, describing the dynamics of Susceptibles and Infected in wildlife diseases, is presented. The two patches are identical in absence of control, and culling activities are performed in only one of them. Firstly, the dynamics of the system in absence of control is investigated. Then, two types of localized culling strategies (proactive end reactive) are considered. The proactive control is modeled by a constant culling effort, and for the ensuing model the disease free equilibrium is characterized and existence of the endemic equilibrium is discussed in terms of a suitable control reproduction number. The localized reactive control is modeled by a piecewise constant culling effort function, that introduces an extra–mortality when the number of infected individuals in the patch overcomes a given threshold. The reactive control is then analytically and numerically investigated in the frame of *Filippov systems*.

We find that localized culling may be ineffective in controlling diseases in wild populations when the infection affects host fecundity in addition to host mortality, even leading to unexpected increases in the number of infected individuals in the nearby areas.

1. **Introduction.** In the last decades, emerging and re–emerging infectious diseases (ERIDs) have been responsible for significant economic and social impacts in both developed [25] and developing countries [34]. Jones *et al.* [33] showed that zoonotic infections originated in wildlife have accounted for the majority of ERID events since the 1940s and are representing a growing threat to global health. As a consequence, actions aiming at controlling diseases in wild populations can provide

2010 *Mathematics Subject Classification.* Primary: 37N25; Secondary: 92D30.

Key words and phrases. SI model, metapopulation, Filippov system, reproduction number, equilibria, stability.

* Corresponding author: Maria Groppi.

benefits on wildlife protection and conservation as well as on the sustainability of agriculture and public health.

However, disease control through vaccination and drug treatments, which represent common intervention measures in human and livestock infections, is often not feasible, or practical, in wildlife because of the lack of resources or the unavailability of suitable diagnostic tools [18]. In these circumstances, non–selective culling, which consists in the slaughtering of both infected and healthy individuals, represents the only available disease control strategy.

The effectiveness of culling relies on the assumption that, under a given threshold of host density, the population becomes too sparse, then, the number of potentially infectious contacts between infected and susceptible individuals become too low to allow the disease to spread and persist in the population [2]. Yet there are empirical evidences suggesting that culling has been ineffective in reducing disease burden in wildlife populations for different infections, such as rabies in canids [37, 46], facial tumor disease in Tasmanian devil [36], and bovine tuberculosis in European badger [27].

The main causes for the failure of culling in the eradication of diseases in wild populations have been ascribed to compensatory mechanisms, such as the density–dependent positive feedbacks on recruitment and dispersal triggered by the excess of mortality due to culling [12, 43]. Specifically, by reducing the host population abundance, culling can reduce the density–dependent constrains on host birth rate, thereby producing a flush in new susceptible individuals in the population [29, 46]. These new susceptibles represent a reservoir for new infections, which nullifies the expected benefits of disease control campaigns or, in some cases, even increases the disease burden in the population [5, 7, 15] or the duration of the epidemic [9, 10].

On the other hand, different studies showed that culling may disrupt the host social structure increasing the animal home range and prompting long–distance movement and dispersal (perturbation hypothesis), thus increasing the probability of potentially infectious contacts between neighboring groups [13, 39, 42]. In particular, studies carried in the British Isles on the effectiveness of localized proactive and reactive culling as measures for bovine tuberculosis (*Mycobacterium bovis*) control in European badger showed that culling led to a decrease in disease burden in the controlled lands, while caused an increase in the infections in the nearby areas [3, 4, 26, 45]. As expected from the perturbation hypothesis, the increase of *M. bovis* prevalence was associated with expanded home ranges and more frequent migration events in badger [4].

In this work, we will consider a metapopulation epidemic mathematical model, described by a system of ODEs for Susceptibles and Infected, with two patches which are identical in absence of control and localized culling control which is performed in only one of them. We will show by means of qualitative analysis and numerical simulations that, also in the absence of the density–dependent compensatory effects on recruitment and dispersal, localized culling may be ineffective in controlling diseases in wild populations and it may even lead to unexpected increases in the number of infected individuals in the nearby areas.

Here, we investigate the effectiveness of localized culling using a metapopulation Susceptibles–Infected (SI) model with density–dependent mortality of the host and disease–induced host sterilization. Disease–induced fecundity reduction (or sterilization) of the host has been frequently observed in host–pathogen interactions. Such kind of disease–induced fecundity reduction of the host has been frequently

observed in host–pathogen interactions. Mathematical models describing the dynamics of fecundity–reducing infections have been developed for rabies – where the fecundity reduction is generated by the severely debilitating nature of the infection and the frenzied behavior induced – in different mammal species [6], cowpox in wild rodents [40], and several infections of invertebrate hosts, such as crustaceans and mollusks [11]. Moreover, we will show that the counter–intuitive effects of culling hold also relaxing the hypotheses of disease–induced host sterility and density–dependent host mortality in the infection model.

2. **The metapopulation mathematical model.** We expand a traditional SI epidemic framework developed for host–sterilizing infections in wild animals to describe the effect of localized proactive and reactive culling on the control of wildlife diseases in a two–patches metapopulation model (see e.g. [2, 5, 19]). From an epidemiological point of view, hosts can be subdivided into compartments with respect to the infection: the susceptible compartments $S_j(t)$ – i.e., healthy individuals that can be infected by the pathogen – and the infected compartments $I_j(t)$ – i.e., diseased individuals that can infect other individuals; subscript $j(= 1, 2)$ defines the patch in the metapopulation to which the epidemiological compartment belongs.

In order to describe localized culling control in the model we assume that culling activities can be performed in one of the two patches only (specifically patch 1), while the other one (patch 2) is uncontrolled. We also assume the two patches are identical in the absence of control, namely the demographic and epidemiological parameters are the same.

Then, the metapopulation model can be represented by the following set of four ordinary differential equations

$$\dot{S}_1 = rS_1 - \gamma S_1 N_1 - \beta S_1 I_1 - cS_1 - DS_1 + DS_2 \tag{1a}$$

$$\dot{I}_1 = \beta S_1 I_1 - (\mu + \alpha + c + \gamma N_1) I_1 - DI_1 + DI_2 \tag{1b}$$

$$\dot{S}_2 = rS_2 - \gamma S_2 N_2 - \beta S_2 I_2 - DS_2 + DS_1 \tag{1c}$$

$$\dot{I}_2 = \beta S_2 I_2 - (\mu + \alpha + \gamma N_2) I_2 - DI_2 + DI_1, \tag{1d}$$

where the upper dot is used to denote the time derivative. $N_j = S_j + I_j$ represents the total host population in patch j. All the parameters are positive constants: $r = \nu - \mu$ represents the intrinsic growth rate, being ν the fertility rate and μ the natural mortality rate; γ and α represent the density–dependent mortality rate of a disease–free host population and the additional mortality rate caused by the infection, respectively; and β represents the transmission rate between infected and susceptible individuals. Moreover, we define D to be the per–capita dispersal rate from a patch to the other; and c to be the culling effort.

In order to analyze the effects of both localized proactive and reactive culling strategies in model (1), we implement two different control functions. Thus, the localized proactive culling strategy in model (1) is obtained by imposing culling effort c to be a constant function

$$c = \bar{c} = const, \tag{2}$$

and the localized reactive culling strategy by imposing culling effort c to be a piecewise constant function as in [20]

$$c = \frac{\bar{c}}{2}[1 + sgn(I_1 - \theta)], \tag{3}$$

where $\bar{c}$ represents the maximum effort enforceable, and θ represents the threshold for the detection of the infection. Expression (3) implies that population N_1 in patch 1 undergoes an extra–mortality $\bar{c}$ due to culling when the number of infected individuals in the patch is higher than threshold θ, while no culling activities are performed when the infection is under the threshold of detection. Therefore, threshold θ introduces a discontinuity, so that model (1) with (3) becomes a discontinuous piecewise–smooth system (also called *Filippov system*) in which sliding motions are possible on the manifold separating the region (in state space) where control is allowed from that where it is not [28].
More precisely, by introducing the so–called *switching manifold*

$$\Sigma = \{(S_1, I_1, S_2, I_2) \in \mathbb{R}^4 : I_1 - \theta = 0\},$$

and denoting with $f^{(1)}$ (resp. $f^{(2)}$) the RHS of model (1) with $c = 0$ (resp. $c = \bar{c}$), then sliding occurs on the *sliding set*

$$\Sigma_s = \{(S_1, I_1, S_2, I_2) \in \Sigma : f_2^{(2)} \leq 0 \leq f_2^{(1)}\}, \tag{4}$$

namely, where the components of two vector fields $f^{(i)}$, $i = 1, 2$, transversal to Σ are 'pushing' in opposite directions, forcing the state of the system to remain on the switching manifold and slide on it. Σ_s terminates in Σ when a *tangency* occurs, i.e. when $f_2^{(1)}$ or $f_2^{(2)}$ vanish, implying that $f^{(1)}$ or $f^{(2)}$ are tangent to the switching manifold. Tangencies are strategically important for bifurcation analysis.
As first pointed out by Filippov, sliding motions obey the ODE system having as RHS the unique convex combination of $f^{(1)}$ and $f^{(2)}$ parallel to Σ_s [28], i.e.,

$$[\dot{S}_1, \dot{I}_1, \dot{S}_2, \dot{I}_2]^T\Big|_{\Sigma_s} = \lambda f^{(1)} + (1 - \lambda) f^{(2)} \tag{5}$$

with

$$\lambda = \frac{(\nabla(I_1 - \theta))^T \cdot f^{(2)}}{(\nabla(I_1 - \theta))^T \cdot \left(f^{(2)} - f^{(1)}\right)}.$$

Equilibrium points of system (5) are called *pseudo–equilibria* for model (1)–(3) and correspond to a stationary sliding solution.
The analysis of planar piecewise–smooth autonomous systems has been widely developed in recent years, see e.g. [31, 35]. However, there is still no obvious classification of the dynamics of higher dimensional piecewise–smooth systems [30]. Then, the behaviors exhibited by model (1) with localized reactive culling (3), which represents a four–dimension piecewise–smooth system, are too complex to be fully investigated analytically. As a consequence, we numerically investigate system (1)–(3) through simulations performed with the event–driven method developed by Piiroinen and Kuznetsov [38] for sliding systems to find model attractors. A bifurcation analysis in the parameter space identified by the reactive control parameters, $\bar{c}$ and θ, has been also performed with SLIDECONT [21], which is a software based on the package AUTO [24] to continue solutions to nonlinear boundary–value problems via orthogonal collocation.

3. **Results.** It can be shown that model (1) is consistent, namely its state variables remain positive for any trajectory starting from positive conditions, as stated by the following theorem:

Theorem 3.1. *If we consider positive initial conditions $S_1(0)$, $I_1(0)$, $S_2(0)$ and $I_2(0)$, then the solutions of the differential system (1) are positive at each time $t > 0$.*

Proof. We shall prove the statement by contradiction.

Let us start by considering the state variables $S_1(t)$ and $S_2(t)$ and let $t_1 > 0$ be the first time instant when $S_1(t)S_2(t) = 0$. Since the initial conditions are positive, the variables S_1 and S_2 (and hence their product) are positive in $[0, t_1)$.

If we assume that $S_1(t_1) = 0$ and $S_2(t_1) \geq 0$, then, by denoting with

$$m = \min_{[0,t_1]}\{r - c - D - \beta I_1(t) - \gamma S_1(t)\},$$

one yields $\dot{S}_1(t) \geq mS_1(t)$ for $t \in [0, t_1]$. Therefore, $S_1(t_1) \geq S_1(0)e^{mt_1} > 0$, that contradicts our assumption. Then, it must be $S_1(t_1) > 0$ and $S_2(t_1) = 0$, which, however, implies that $\dot{S}_2(t_1) > 0$, namely $S_2(t)$ must be negative just before t_1. Thus, the existence of t_1 is definitely excluded.

With the same arguments one can prove the positivity of the infected state variables $I_1(t)$ and $I_2(t)$. □

3.1. **Metapopulation model without control.** Before exploring the effects of localized proactive and reactive culling on the infection dynamics, we analyze the main features of model (1), deriving the equilibria in the absence of control ($c = 0$) and the expression for the basic reproduction number, $\mathcal{R}_0$ (which corresponds to the average number of secondary infections caused by a single primary infection in a totally susceptible population at the disease–free equilibrium).
In the absence of control ($c = 0$), model (1) assumes a symmetric form, which allows us to prove that:

Theorem 3.2. *If $c = 0$ in model (1), then at any equilibrium point the size of the susceptible (resp. infected) compartment in patch 1 is equal to the size of the susceptible (resp. infected) compartment in patch 2.*

Proof. Let us consider the algebraic system obtained by setting the RHS of model (1), with $c = 0$, equal to zero, namely:

$$rS_1 - \gamma S_1 N_1 - \beta S_1 I_1 - DS_1 + DS_2 = 0 \tag{6a}$$
$$\beta S_1 I_1 - (\mu + \alpha + \gamma N_1)I_1 - DI_1 + DI_2 = 0 \tag{6b}$$
$$rS_2 - \gamma S_2 N_2 - \beta S_2 I_2 - DS_2 + DS_1 = 0 \tag{6c}$$
$$\beta S_2 I_2 - (\mu + \alpha + \gamma N_2)I_2 - DI_2 + DI_1 = 0. \tag{6d}$$

By contradiction, we assume that there exists a positive solution to system (6), say $[\bar{S}_1, \bar{I}_1, \bar{S}_2, \bar{I}_2]$, such that $\bar{S}_1 \neq \bar{S}_2$ or $\bar{I}_1 \neq \bar{I}_2$, possibly being both valid. Denote with $\bar{N}_i = \bar{S}_i + \bar{I}_i$, $i = 1, 2$. Then, two cases must be considered:

- $\bar{I}_1 = \bar{I}_2$ If $\bar{S}_1 > \bar{S}_2$, then from (6a) and (6c) it follows that
$$r - \gamma\bar{N}_1 - \beta\bar{I}_1 > 0 > r - \gamma\bar{N}_2 - \beta\bar{I}_2, \tag{7}$$
which reduce to $\bar{N}_1 < \bar{N}_2$ and a contradiction arises.
A similar argument applies if $\bar{S}_2 > \bar{S}_1$.
- $\bar{I}_1 \neq \bar{I}_2$ In order to fix the ideas, let us assume $\bar{I}_1 > \bar{I}_2$ (the opposite case follows in analogous way).
If $\bar{S}_1 > \bar{S}_2$, then, analogously to what happens if $\bar{I}_1 = \bar{I}_2$, the inequalities (7) reduce to $\gamma\bar{N}_1 + \beta\bar{I}_1 < \gamma\bar{N}_2 + \beta\bar{I}_2$, which is in contrast with the assumptions $\bar{S}_1 > \bar{S}_2$, $\bar{I}_1 > \bar{I}_2$.
Otherwise, if $0 < \bar{S}_1 \leq \bar{S}_2$, then, the inequalities (7) must be reversed, namely
$$r - \gamma\bar{N}_2 - \beta\bar{I}_2 \geq 0 \geq r - \gamma\bar{N}_1 - \beta\bar{I}_1, \tag{8}$$

yielding:

$$\gamma\bar{N}_2 + \beta\bar{I}_2 \leq \gamma\bar{N}_1 + \beta\bar{I}_1. \tag{9}$$

On the other hand, by handling the (6b) and (6d), one obtains

$$(\beta\bar{S}_1 - (\mu + \alpha + \gamma\bar{N}_1))\bar{I}_1 > 0 > (\beta\bar{S}_2 - (\mu + \alpha + \gamma\bar{N}_2))\bar{I}_2, \tag{10}$$

which, for the positivity of the $\bar{I}_i$, $i = 1, 2$, reduce to

$$\gamma(\bar{N}_1 - \bar{N}_2) < \beta(\bar{S}_1 - \bar{S}_2). \tag{11}$$

Being $\bar{S}_1 \leq \bar{S}_2$, the last inequality implies that $\bar{N}_1 < \bar{N}_2$. However, adding the (9) and (11) leads to a contradiction: $\bar{N}_1 > \bar{N}_2$.

In conclusion, if $\bar{S}_1 = \bar{S}_2 = 0$, then the (10) are still valid and reduce to $\bar{I}_1 < \bar{I}_2$, which is again in contrast with the initial assumption.

□

In other words, in searching model equilibria, it is not restrictive to assume the two patches are identical. In particular, model (1) with $c = 0$ has always a trivial equilibrium, $E_0 = [0, 0, 0, 0]$, and a disease–free equilibrium, $E_1 = [K, 0, K, 0]$, where

$$K = \frac{r}{\gamma} \tag{12}$$

represents the carrying capacity for a disease–free host population. It is easy to prove that E_0 is always unstable if $r > 0$, while E_1 is asymptotically stable if and only if the basic reproduction number of model (1), $\mathcal{R}_0$, is lower than 1 [1].

The basic reproduction number can be calculated as the spectral radius of the *next generation* matrix, $\mathcal{R}_0 = \rho(FV^{-1})$, where F and V are defined as Jacobian matrices of the new infections appearance and the other rates of transfer, respectively, calculated for infected compartments at model (1) disease–free equilibrium [22, 44]. Then, model (1) basic reproduction number can be defined as

$$\mathcal{R}_0 = \frac{\beta K}{\mu + \alpha + r}, \tag{13}$$

with K given in (12) and coincides with that for the corresponding homogeneous mixing model. When $\mathcal{R}_0 > 1$ in equation (13), the disease–free equilibrium is unstable and there exists a unique asymptotically stable positive endemic equilibrium, called $E_2 = [\bar{S}, \bar{I}, \bar{S}, \bar{I}]$, where

$$\bar{S} = \frac{\mu + \alpha + \gamma\bar{N}}{\beta} \tag{14a}$$

$$\bar{I} = \frac{r - \gamma\bar{N}}{\beta} \tag{14b}$$

with

$$\bar{N} = \frac{r + \mu + \alpha}{\beta}. \tag{15}$$

We notice that expressions (14), defining the endemic equilibrium in (1) for $c = 0$, correspond to the endemic equilibrium for the associated homogeneous mixing model (see [2], under the assumption of negligible incubation period) and stability properties follow straightforwardly.

Note also that necessary condition for being $\bar{I}$ positive is that

$$\beta > \gamma,$$

hence we assume it always fulfilled in the following.

3.2. **The effect of localized proactive culling.** Analyzing metapopulation model (1)–(2) – i.e., with localized proactive culling strategy –, we find that there always exists a trivial equilibrium, $E_0^{\bar{c}} = [0, 0, 0, 0]$. Conversely than the case with $c = 0$, the trivial equilibrium $E_0^{\bar{c}}$ is not always unstable when $r > 0$. Indeed, linearization of system (1)–(2) around $E_0^{\bar{c}}$ leads to $E_0^{\bar{c}}$ locally asymptotically stable if and only if

$$D > r \quad \text{and} \quad \bar{c} > \hat{c} = \frac{r(2D - r)}{D - r}, \tag{16}$$

as can be proved by Sylvester criterion [32], being the Jacobian matrix of system (1)–(2) evaluated at $E_0^{\bar{c}}$ a symmetric matrix.

Expression (16) suggests that, for frequent dispersers (i.e., species with $D > r$, as defined in [14]), sufficiently high levels of constant culling efforts ($\bar{c} > \hat{c}$) in one of the patches can lead to the extinction of the entire population.

When expression (16) is not satisfied, the trivial equilibrium is unstable and there exists a positive disease–free equilibrium, $E_1^{\bar{c}}$, as stated by the following theorem:

Theorem 3.3. *If condition (16) is not verified, then model (1)–(2) admits an unique positive disease–free equilibrium* $E_1^{\bar{c}} = [\hat{K}_1, 0, \hat{K}_2, 0]$ *and* $0 < \hat{K}_1 \leq \hat{K}_2$.

Proof. Denote the generic disease–free equilibrium equilibrium of model (1)–(2) by $E_1^{\bar{c}} = [\hat{K}_1, 0, \hat{K}_2, 0]$, where $\hat{K}_1$, $\hat{K}_2 > 0$. The components $\hat{K}_1$, $\hat{K}_2$ are the solutions of the algebraic system obtained by setting the RHS of equations (1a) and (1c), with $c = \bar{c}$, equal to zero, namely:

$$\begin{aligned} (r - \bar{c} - D)\hat{K}_1 - \gamma\hat{K}_1^2 + D\hat{K}_2 = 0 \\ (r - D)\hat{K}_2 - \gamma\hat{K}_2^2 + D\hat{K}_1 = 0, \end{aligned} \tag{17}$$

yielding the admissibility condition:

$$\hat{K}_1 = \frac{D - r + \gamma\hat{K}_2}{D}\hat{K}_2 > 0 \iff \hat{K}_2 > \frac{r - D}{\gamma}. \tag{18}$$

Substituting the expression of $\hat{K}_1$ into (17), one obtains $\hat{K}_2 \neq 0$ as solution of

$$f(\hat{K}_2) = 0, \tag{19}$$

with

$$f(\hat{K}_2) = a_0 + a_1\hat{K}_2 + a_2\hat{K}_2^2 + a_3\hat{K}_2^3,$$

and

$$\begin{aligned} a_0 &= D(\bar{c}(D - r) - r(2D - r)) \\ a_1 &= \gamma(\bar{c}D + (D - r)(2D - r)) \\ a_2 &= 2\gamma^2(D - r) \\ a_3 &= \gamma^3 > 0. \end{aligned}$$

Let us differentiate the equation (19), yielding:

$$f'(\hat{K}_2) = a_1 + 2a_2\hat{K}_2 + 3a_3\hat{K}_2^2 = 0,$$

whose discriminant is $\Delta = a_2^2 - 3a_1a_3 = -3\bar{c}D - 2D^2 + Dr + r^2$. If $\Delta \leq 0$, then f is an increasing function. Otherwise, if $\Delta > 0$, then (3.3) admits two real solutions:

$$\hat{K}_{2\pm} = \frac{2(r - D) \pm \sqrt{\Delta}}{3\gamma},$$

that are relative minimum/maximum points for f and it is straightforward to check that

$$\hat{K}_{2-} < \frac{r-D}{\gamma}.$$

In any case, we have

$$f\left(\frac{r-D}{\gamma}\right) = -D^3 \leq 0.$$

Thus, exactly one root of (19) satisfies the admissibility condition (18). If $D > r$, it is not obvious that such a root is positive: one can easily check that $a_0 = f(0)$ is (resp. is not) positive if expression (16) is (resp. is not) fulfilled. Hence, in summary, system (1)–(2) admits an unique disease–free equilibrium $E_1^{\bar{c}}$ if condition (16) is not satisfied; there are none if (16) is verified.

To conclude the proof, we have to prove that, when the disease–free equilibrium $E_1^{\bar{c}}$ exists, $\hat{K}_1 \leq \hat{K}_2$ or, equivalently, $\hat{K}_2 \leq r/\gamma$ (from (18)). Being $f(r/\gamma) = cD^2 \geq 0$, the last inequality always holds. □

Thus, in the presence of localized proactive culling the disease–free equilibrium becomes $E_1^{\bar{c}} = [\hat{K}_1, 0, \hat{K}_2, 0]$, where $\hat{K}_1$ and $\hat{K}_2$ can not be easily written explicitly, since they come from solutions of the third–order equation (19).

When proactive culling as in (2) is implemented in model (1), we can compute through the *next generation* matrix method the control reproduction number, $\mathcal{R}_C$, similarly to $\mathcal{R}_0$. The control reproduction number is defined as the average number of secondary infections produced by a single infected individual in a susceptible population at its disease–free equilibrium experiencing culling effort $\bar{c}$. Its expression is

$$\mathcal{R}_C = \frac{1}{2}\beta \frac{\hat{K}_1\,(\mu+\alpha+D) + \hat{K}_2(\mu+\alpha+\bar{c}+D) + 2\gamma\hat{K}_1\hat{K}_2 + \sqrt{\Delta_C}}{\left(\mu+\alpha+\bar{c}+\gamma\hat{K}_1+D\right)\left(\mu+\alpha+\gamma\hat{K}_2+D\right) - D^2}, \tag{20}$$

with

$$\begin{aligned}\Delta_C =& \hat{K}_1^2(\mu+\alpha+D)^2 + \hat{K}_2^2(\mu+\alpha+\bar{c}+D)^2 + \\ &+ 2\hat{K}_1\hat{K}_2\left[2D^2 - (\mu+\alpha+\bar{c}+D)(\mu+\alpha+D)\right]\end{aligned} \tag{21}$$

(for details see Appendix A). When it exists, disease–free equilibrium $E_1^{\bar{c}}$ is asymptotically stable if and only if the control reproduction number $\mathcal{R}_C$ in (20) is lower than 1; on the other hand, if $\mathcal{R}_C > 1$ the disease–free equilibrium is unstable [22, 44].

As far as the existence and the number of model endemic equilibria, an analytical investigation is very hard to perform. Therefore, numerical analyses are carried out to understand the effect of localized proactive culling on the disease dynamics. Extensive numerical tests suggest that there are no endemic equilibria when $\mathcal{R}_C < 1$; otherwise, when $\mathcal{R}_C > 1$, there exists an unique asymptotically stable endemic equilibrium, say $E_2^{\bar{c}} = [\hat{S}_1, \hat{I}_1, \hat{S}_2, \hat{I}_2]$.

In Fig. 1 we show the effect of the host dispersal rate (D) and the localized proactive culling effort ($\bar{c}$) on the existence and stability of model (1)–(2) equilibria through bifurcation analysis [41]. The curve TC_0 defines a transcritical bifurcation representing the threshold for host extinction (in (16)) that separates the region in which the total host population goes extinct from the region in which model (1)–(2) converges toward a disease–free equilibrium. The curve TC_1 defines a transcritical bifurcation representing the threshold for infection establishment ($\mathcal{R}_C = 1$) that

separates the region in which the pathogen fails to establish itself (disease–free equilibrium) from the region in which the pathogen is able to invade the host population and model (1)–(2) converges toward an endemic equilibrium.

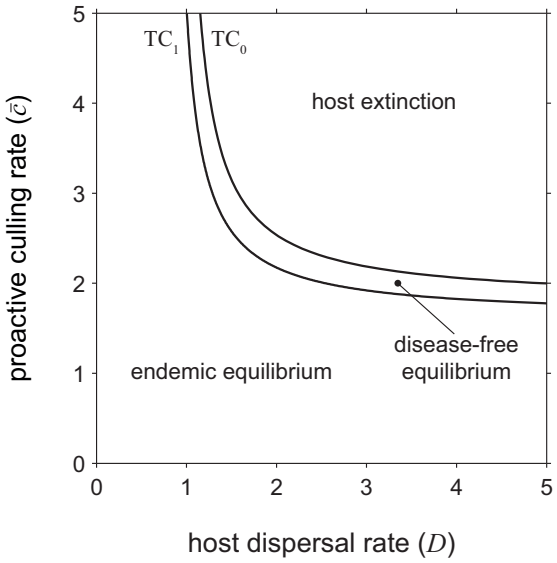

FIGURE 1. The effects of variation in host dispersal rate (D) and localized proactive culling effort ($\bar{c}$) on model (1)–(2) behaviors. The curves TC_0 (i.e., $\bar{c} = \hat{c}$ in (16)) and TC_1 (i.e., $\mathcal{R}_C = 1$), which represent transcritical bifurcations, delimit three different regions in the parameter space $[D, \bar{c}]$ where system (1), in the presence of localized proactive culling (2), converges to host extinction, disease–free equilibrium, or endemic equilibrium. Parameter values for model (1)–(2) have been fixed to: $r = 0.9$; $\mu = 0.2$; $K = 600$; $\alpha = 0$; $\mathcal{R}_0 = 10$ (or rather $\beta = 0.01833$, see (13)).

We investigate the effectiveness of localized proactive culling (2) in successfully control infectious diseases in wildlife by analysing the variation of susceptible and infected individuals as a function of $\bar{c}$ at endemic equilibrium $E_2^{\bar{c}}$ in model (1)–(2). Most of all, we are interested in understanding whether localized proactive culling, $\bar{c}$, can reduce the number of infected individuals both in the culling area ($\hat{I}_1$ in patch 1) and in the neighbouring areas ($\hat{I}_2$ in patch 2). Firstly, we provide analytical results on the variation of $\hat{S}_j$ and $\hat{I}_j$ (with $j = 1, 2$) with respect to $\bar{c}$. In particular, we show that $d\hat{I}_2/d\bar{c}|_{\bar{c}=0}$ can be positive for suitable ecological and epidemiological conditions (see Theorem 3.4). Secondly, since endemic equilibrium $E_2^{\bar{c}}$ is too complex to be computed analytically for strictly positive values of $\bar{c}$, we simulate numerically the number of infected individuals at endemic equilibrium $E_2^{\bar{c}}$ for different values of localized proactive culling, $\bar{c}$.

Theorem 3.4. *The number of infected individuals in patch 1 (I_1) at endemic equilibrium of model (1)–(2), as function of $\bar{c}$, is maximum in $\bar{c} = 0$; namely, $\hat{I}_1(\bar{c}) < \hat{I}_1(0) = \bar{I}$, $\forall \bar{c} > 0$.*

Proof. By considering equations (1) evaluated at equilibrium $E_2^{\bar{c}} = [\hat{S}_1, \hat{I}_1, \hat{S}_2, \hat{I}_2]$ and at equilibrium $E_2 = [\bar{S}, \bar{I}, \bar{S}, \bar{I}]$, as given in (14), and subtracting side by side, one obtains:

$$(\beta+\gamma)\left(\hat{I}_1(\bar{c})-\bar{I}\right)+\bar{c} = -\gamma\left(\hat{S}_1(\bar{c})-\bar{S}\right)+D\left[\frac{\hat{S}_2(\bar{c})}{\hat{S}_1(\bar{c})}-1\right] \tag{22a}$$

$$(\beta-\gamma)\left(\hat{S}_1(\bar{c})-\bar{S}\right) = \bar{c}+\gamma\left(\hat{I}_1(\bar{c})-\bar{I}\right)-D\left[\frac{\hat{I}_2(\bar{c})}{\hat{I}_1(\bar{c})}-1\right] \tag{22b}$$

$$(\beta+\gamma)\left(\hat{I}_2(\bar{c})-\bar{I}\right) = -\gamma\left(\hat{S}_2(\bar{c})-\bar{S}\right)+D\left[\frac{\hat{S}_1(\bar{c})}{\hat{S}_2(\bar{c})}-1\right] \tag{22c}$$

$$(\beta-\gamma)\left(\hat{S}_2(\bar{c})-\bar{S}\right) = \gamma\left(\hat{I}_2(\bar{c})-\bar{I}\right)-D\left[\frac{\hat{I}_1(\bar{c})}{\hat{I}_2(\bar{c})}-1\right]. \tag{22d}$$

By contradiction, we assume that there exists a $\bar{c}_0 > 0$ such that $\hat{I}_1(\bar{c}_0) \geq \bar{I}$. Then, signs in (22b) impose that at least one of the following inequalities holds:

- $\hat{I}_2(\bar{c}_0) > \hat{I}_1(\bar{c}_0)$. Then, $\hat{I}_2(\bar{c}_0) > \bar{I}$ and addenda signs in (22c) and (22d) impose that $\hat{S}_1(\bar{c}_0) > \hat{S}_2(\bar{c}_0) > \bar{S}$. However, a contradiction in (22a) arises.
- $\hat{S}_1(\bar{c}_0) > \bar{S}$. From sign of equations (22a) and (22c) one yields $\hat{S}_2(\bar{c}_0) > \hat{S}_1(\bar{c}_0) > \bar{S}$ and $\hat{I}_1(\bar{c}_0) \geq \bar{I} > \hat{I}_2(\bar{c}_0)$, respectively. This leads to a contradiction in (22d).

Thus, it must be $\hat{I}_1(\bar{c}) < \bar{I}$, $\forall \bar{c} > 0$. □

Theorem 3.5. *$\forall \bar{c} > 0$, the number of infected individuals in patch 1 at endemic equilibrium $E_2^{\bar{c}}$ of model (1)–(2) is smaller than the corresponding number of infected individuals in patch 2 (I_2); namely, $\hat{I}_1(\bar{c}) < \hat{I}_2(\bar{c})$, $\forall \bar{c} > 0$.*

Proof. By contradiction, we assume that there exists a $\bar{c}_0 > 0$ such that $\hat{I}_1(\bar{c}_0) \geq \hat{I}_2(\bar{c}_0)$. Then, from (22c) and (22d) and in virtue of Theorem 3.4, one yields $\hat{S}_1(\bar{c}_0) < \hat{S}_2(\bar{c}_0) < \bar{S}$. On the other hand, by handling equations (1b)–(1d) at endemic equilibrium $E_2^{\bar{c}_0}$ and subtracting side by side, we obtain

$$(\beta-\gamma)(\hat{S}_1-\hat{S}_2)-\bar{c}_0-\gamma(\hat{I}_1-\hat{I}_2)+D\left(\frac{\hat{I}_2}{\hat{I}_1}-\frac{\hat{I}_1}{\hat{I}_2}\right)=0,$$

which is in contradiction with addenda signs. Hence, it must be $\hat{I}_1(\bar{c}) < \hat{I}_2(\bar{c})$, $\forall \bar{c} > 0$. □

Theorem 3.6. *The derivative of the number of susceptible individuals in patch 2 (S_2) with respect to $\bar{c}$, at endemic equilibrium of model (1)–(2), is always positive when $\bar{c} = 0$. Instead, the derivative of the number of infected individuals in patch 2 is positive when $\bar{c} = 0$ if and only if the following condition holds:*

$$\left.\frac{d\hat{I}_2}{d\bar{c}}\right|_{\bar{c}=0} > 0 \iff \frac{2D}{r} < \frac{\mathcal{R}_0-2}{\mathcal{R}_0}, \tag{23}$$

with $\mathcal{R}_0$ defined in (13).

Proof. By differentiating with respect to $\bar{c}$ the RHS side of equations (1) at endemic equilibrium $E_2^{\bar{c}}$, we obtain

$$\begin{aligned}\beta\hat{I}_1^{'}(\bar{c}) =& -1-\gamma\hat{S}_1^{'}(\bar{c})-\gamma\hat{I}_1^{'}(\bar{c}) \\ &+\frac{D}{\hat{S}_1^2(\bar{c})}[\hat{S}_2^{'}(\bar{c})\hat{S}_1(\bar{c})-\hat{S}_1^{'}(\bar{c})\hat{S}_2(\bar{c})] \end{aligned} \tag{24a}$$

$$\beta\hat{S}_1^{'}(\bar{c}) =1+\gamma\hat{S}_1^{'}(\bar{c})+\gamma\hat{I}_1^{'}(\bar{c})-\frac{D}{\hat{I}_1^2(\bar{c})}[\hat{I}_2^{'}(\bar{c})\hat{I}_1(\bar{c})-\hat{I}_1^{'}(\bar{c})\hat{I}_2(\bar{c})] \tag{24b}$$

$$\beta\hat{I}_2^{'}(\bar{c}) =-\gamma\hat{S}_2^{'}(\bar{c})-\gamma\hat{I}_2^{'}(\bar{c})+\frac{D}{\hat{S}_2^2(\bar{c})}[\hat{S}_1^{'}(\bar{c})\hat{S}_2(\bar{c})-\hat{S}_2^{'}(\bar{c})\hat{S}_1(\bar{c})] \tag{24c}$$

$$\beta\hat{S}_2^{'}(\bar{c}) =\gamma\hat{S}_2^{'}(\bar{c})+\gamma\hat{I}_2^{'}(\bar{c})-\frac{D}{\hat{I}_2^2(\bar{c})}[\hat{I}_1^{'}(\bar{c})\hat{I}_2(\bar{c})-\hat{I}_2^{'}(\bar{c})\hat{I}_1(\bar{c})]. \tag{24d}$$

When $\bar{c}=0$, $\hat{S}_j(0)=\bar{S}$ and $\hat{I}_j(0)=\bar{I}$, with $\bar{S}$ and $\bar{I}$ defined as in (14). Then – by substituting the expressions for $\hat{I}_1^{'}(0)$ and $\hat{I}_2^{'}(0)$ (derived in (24a) and (24c), respectively) as functions of $\hat{S}_1^{'}(0)$ and $\hat{S}_2^{'}(0)$ –, we can re–write (24b) and (24d) as follows:

$$A(\bar{S},\bar{I})\hat{S}_1^{'}(0)=\beta-\frac{D}{\bar{I}}+B(\bar{S},\bar{I})\hat{S}_2^{'}(0) \tag{25a}$$

$$A(\bar{S},\bar{I})\hat{S}_2^{'}(0)=\frac{D}{\bar{I}}+B(\bar{S},\bar{I})\hat{S}_1^{'}(0), \tag{25b}$$

where

$$A(\bar{S},\bar{I})=\beta^2+B(\bar{S},\bar{I}), \tag{26}$$

and

$$B(\bar{S},\bar{I})=\gamma\frac{D}{\bar{I}}+\gamma\frac{D}{\bar{S}}+2\frac{D^2}{\bar{S}\bar{I}}. \tag{27}$$

By substituting (25a) in (25b) and rearranging, we find the equation

$$\frac{A^2-B^2}{A}\hat{S}_2^{'}(0)=\beta\frac{B}{A}+\left(1-\frac{B}{A}\right)\frac{D}{\bar{I}}.$$

Being $A(\bar{S},\bar{I})>B(\bar{S},\bar{I})$, condition $\hat{S}_2^{'}(0)>0$ is always satisfied.
In a similar way, we prove the second part of the statement. By substituting the expressions for $\hat{S}_1^{'}(0)$ and $\hat{S}_2^{'}(0)$ (derived in (24b) and (24d), respectively) as functions of $\hat{I}_1^{'}(0)$ and $\hat{I}_2^{'}(0)$, we can re–write (24a) and (24c) as follows:

$$A(\bar{S},\bar{I})\hat{I}_1^{'}(0)=-\beta-\frac{D}{\bar{S}}+B(\bar{S},\bar{I})\hat{I}_2^{'}(0) \tag{28a}$$

$$A(\bar{S},\bar{I})\hat{I}_2^{'}(0)=\frac{D}{\bar{S}}+B(\bar{S},\bar{I})\hat{I}_1^{'}(0), \tag{28b}$$

where functions A and B are given in (26) and (27), respectively. By substituting (28a) in (28b) and rearranging, we find the equation

$$\frac{A^2-B^2}{A}\hat{I}_2^{'}(0)=-\beta\frac{B}{A}+\left(1-\frac{B}{A}\right)\frac{D}{\bar{S}}. \tag{29}$$

Hence, condition $\hat{I}_2^{'}(0)>0$ is fulfilled if and only if the RHS of (29) is positive (i.e., if $\beta D-B(\bar{S},\bar{I})\bar{S}>0$). With simple algebraic manipulations – and remembering equalities (13) and (14) – then yields to

$$\frac{2D}{r}<\frac{\mathcal{R}_0-2}{\mathcal{R}_0}.$$

□

Proposition 1. *In the limit case $D \to 0$, the derivative of the number of susceptible individuals in patch 1 (S_1) with respect to $\bar{c}$, at endemic equilibrium $E_2^{\bar{c}}$ of model (1)–(2), converges to $1/\beta$.*

Proof. It is an immediate consequence of equations (24a) and (24b). □

From expression (23), we notice that necessary conditions for localized proactive culling to increase (instead of decrease) the number of infected individuals in patch 2 are: $2D < r$ (i.e., hosts are very infrequent dispersers) and $\mathcal{R}_0 > 2$ (i.e., in the corresponding uncontrolled model the first infected individual can, on average, infect more than two individuals).

Remark 1. In the case the total host population at endemic equilibrium for $c = 0$ (15) is much lower than the carrying capacity K, the effect of the density–dependent mortality rate at the endemic equilibrium is negligible, which corresponds to assume $\gamma \to 0$. In this scenario, it is straightforward to check that condition (23) for being $\hat{I}_2'(0) > 0$ reduces to: $2D < r$. Instead, if, in addition to setting $\gamma \to 0$, we also relax the hypothesis of disease–induced sterility (see Appendix B), then such a condition becomes slightly more complex:

$$(\alpha - r)\left(1 - \frac{2D}{r}\right) - (\mu + r) - \frac{\mu + r}{\mu + \alpha}\left(r\frac{\mu + r}{\alpha - r} + 2D\right) > 0, \tag{30}$$

where $\alpha > r$ (which represents the necessary condition for the existence of the endemic equilibrium in the absence of control, see Appendix B). However, once again, formula (30) indicates that having $2D < r$ is necessary for proactive culling to increase the endemic value of infected in the uncontrolled patch.

To investigate more deeply the counter–intuitive result obtained in Theorem 3.6, we numerically compute the parameter conditions for which the number of infected individuals in patch 2 at the endemic equilibrium is higher in the presence of localized proactive control than with the do–nothing alternative (i.e., $\hat{I}_2(\bar{c}) > \bar{I}$). The numerical analyses presented here are performed by exploring the effects of different values of host dispersal (D), proactive culling effort ($\bar{c}$), and disease basic reproduction number of model (1) with $c = 0$ ($\mathcal{R}_0$, given by (13)) on control effectiveness and by keeping the host demographic parameters constant in the simulations. Specifically, we set the host demographic parameters as in [5].

In Fig. 2 we show the parametric regions where condition $\hat{I}_2(\bar{c}) > \bar{I}$ is satisfied for different values of basic reproduction number of the corresponding uncontrolled model ($\mathcal{R}_0$) in the parameter space $[D, \bar{c}]$. Fig. 2 highlights that for low values of host dispersal rates (D), localized culling is ineffective in reducing the infection outside the control zone (i.e., $\hat{I}_2(\bar{c}) > \bar{I}$) for a wide range of culling rate values, also when the basic reproduction number is relatively low.

The dynamics of infected individuals in patch 2 corresponding to the parameter space along the thin dotted line in Fig. 2 is illustrated in Fig. 3. In particular, in Fig. 3 we show the relative variation of the number of infected individuals in patch 2 at endemic equilibrium $E_2^{\bar{c}}$ with respect to the number of infected in the absence of control (i.e., $\delta\hat{I}_2 = (\hat{I}_2 - \bar{I})/\bar{I}$) as a function of the localized proactive culling rate ($\bar{c}$) for an infrequent disperser host ($D/r = 0.1$) and for different values of $\mathcal{R}_0$.

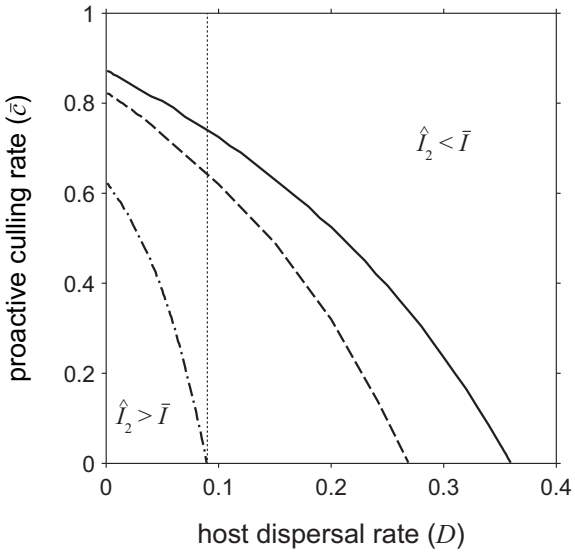

FIGURE 2. Curves in the parameter space $[D, \bar{c}]$ separating the regions in which condition $\hat{I}_2(\bar{c}) > \bar{I}$ or condition $\hat{I}_2(\bar{c}) < \bar{I}$ are satisfied for different values of the basic reproduction number of model (1) with $c = 0$ ($\mathcal{R}_0$, given by (13)). Solid thick curve: $\mathcal{R}_0 = 10$; dashed thick curve: $\mathcal{R}_0 = 5$; dot–dashed thick curve: $\mathcal{R}_0 = 2.5$. The dynamics of infected individuals in patch 2 ($\hat{I}_2$) corresponding to the parameter space along the thin dotted line ($D = 0.1r$) is illustrated in Fig. 3. Unspecified parameters as in Fig. 1.

3.3. **The effect of localized reactive culling.** Let us consider model (1) with the piecewise constant function (3) representing the culling effort in the localized reactive control strategy. We are interested in investigating the long term dynamics of model solutions and, in particular, of sliding motions, occurring on the sliding set (4). To this aim, the following results concerning the existence and stability of stationary sliding solutions (also called pseudo–equilibria) can be proved:

Theorem 3.7. *Necessary condition for the existence of pseudo–equilibria for model (1)–(3) is that*

$$\hat{I}_1 \leq \theta \leq \bar{I}, \tag{31}$$

where $\hat{I}_1$ (resp. $\bar{I}$) is the number of infected individuals in patch 1 at endemic equilibrium $E_2^{\bar{c}}$ (resp. E_2) of model (1) with $c = \bar{c}$ (resp. $c = 0$).

Proof. Firstly note that Theorem 3.4 ensures that $\hat{I}_1 \leq \bar{I}$.
By definition, a pseudo–equilibrium of model (1)–(3) is an equilibrium for system (5) belonging to the sliding set Σ_s (given in (4)), i.e. such that $I_1 = \theta$, and S_1, S_2, I_2 satisfy

$$(r + \mu + \alpha)S_1 - \beta S_1^2 - \beta\theta S_1 - D\frac{I_2}{\theta}S_1 + DS_2 = 0 \tag{32a}$$

$$rS_2 - \gamma S_2 N_2 - \beta S_2 I_2 - DS_2 + DS_1 = 0 \tag{32b}$$

$$\beta S_2 I_2 - (\mu + \alpha + \gamma N_2)I_2 - DI_2 + D\theta = 0, \tag{32c}$$

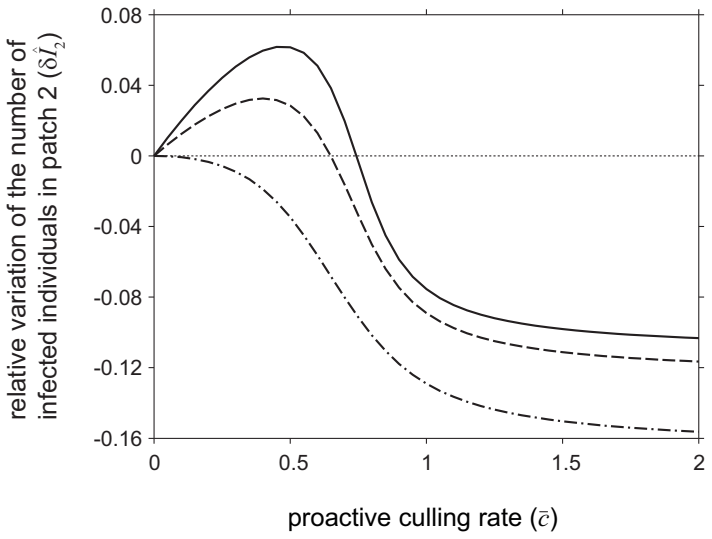

FIGURE 3. Relative variation of the number of infected individuals in patch 2 at endemic equilibrium $E_2^{\bar{c}}$ with respect to the number of infected in the absence of control (i.e., $\delta\hat{I}_2 = (\hat{I}_2 - \bar{I})/\bar{I}$) as a function of the localized proactive culling rate ($\bar{c}$) for a very infrequent disperser host species ($D/r = 0.1$). Solid thick curve: $\mathcal{R}_0 = 10$; dashed thick curve: $\mathcal{R}_0 = 5$; dot–dashed thick curve: $\mathcal{R}_0 = 2.5$. The thin dotted line represents the condition $\hat{I}_2 = \bar{I}$. Unspecified parameters as in Fig. 1.

with

$$(\beta - \gamma)S_1 \geq \mu + \alpha + \gamma\theta + D - D\frac{I_2}{\theta} \tag{33a}$$

$$(\beta - \gamma)S_1 \leq \mu + \alpha + \gamma\theta + \bar{c} + D - D\frac{I_2}{\theta}. \tag{33b}$$

By contradiction, we assume that one of the following inequalities holds:

- $\theta < \hat{I}_1$. Then – by handling the inequality (33b) and equation (1b) at equilibrium $E_2^{\bar{c}}$ –, one yields

$$(\beta - \gamma)(S_1 - \hat{S}_1) - \gamma(\theta - \hat{I}_1) + D\left(\frac{I_2}{\theta} - \frac{\hat{I}_2}{\hat{I}_1}\right) \leq 0,$$

  implying that two mutually–exclusive conditions must be considered:
  - $S_1 < \hat{S}_1$. Then, $N_1 = S_1 + \theta < \hat{S}_1 + \hat{I}_1 = \hat{N}_1$ and by substituting the expression for $\mu + \alpha - DI_2/\theta$ derived from (32a) in (33b) and rearranging, we obtain

$$r - \beta\theta - \gamma N_1 - \bar{c} - D\left(1 - \frac{S_2}{S_1}\right) \leq 0.$$

Subtracting the latter inequality and equation (1a) at equilibrium $E_2^{\bar{c}}$ side by side yields

$$\beta(\theta - \hat{I}_1) + \gamma(N_1 - \hat{N}_1) + D\left(\frac{\hat{S}_2}{\hat{S}_1} - \frac{S_2}{S_1}\right) \geq 0,$$

implying $\hat{S}_2/\hat{S}_1 > S_2/S_1$ and, in particular, $\hat{S}_2 > S_2$.
Let us consider now equations (32b)–(32c) and (1c)–(1d) at equilibrium $E_2^{\bar{c}}$ and subtract side by side, yielding:

$$(\beta + \gamma)\left(I_2 - \hat{I}_2\right) = -\gamma\left(S_2 - \hat{S}_2\right) + D\left(\frac{S_1}{S_2} - \frac{\hat{S}_1}{\hat{S}_2}\right) \tag{34a}$$

$$(\beta - \gamma)\left(S_2 - \hat{S}_2\right) = \gamma\left(I_2 - \hat{I}_2\right) - D\left(\frac{\theta}{I_2} - \frac{\hat{I}_1}{\hat{I}_2}\right). \tag{34b}$$

Sign of (34a) RHS imposes that $I_2 > \hat{I}_2$, which, however, is in contrast with (34b).

- $S_1 \geq \hat{S}_1$, $I_2/\theta < \hat{I}_2/\hat{I}_1$. Then, $I_2 < \hat{I}_2$ and sign of (34b) RHS implies that $S_2 > \hat{S}_2$, which is in contradiction with (34a).

- $\theta > \bar{I}$. Then – by remembering inequality (33a) and equation (1b) at equilibrium E_2 –, one yields

$$(\beta - \gamma)(S_1 - \bar{S}) - \gamma(\theta - \bar{I}) + D\left(\frac{I_2}{\theta} - 1\right) \geq 0,$$

hence at least one between the first and the last addendum must be positive; namely, we consider two alternative cases:

- $S_1 > \bar{S}$. Then, $N_1 > \bar{S} + \bar{I} = \bar{N}$ and by substituting the expression for $\mu + \alpha - DI_2/\theta$ derived from (32a) in (33a) and rearranging, one obtains

$$r - \gamma N_1 - D\left(1 - \frac{S_2}{S_1}\right) \geq \beta\theta.$$

Being $\theta > \bar{I}$, with $\bar{I}$ given in (14b), then $S_2 > S_1 > \bar{S}$.
Accounting now for equations (32b)–(32c) and (1c)–(1d) at equilibrium E_2 and subtracting side by side, yields:

$$(\beta + \gamma)\left(I_2 - \bar{I}\right) = -\gamma\left(S_2 - \bar{S}\right) + D\left(\frac{S_1}{S_2} - 1\right) \tag{35a}$$

$$(\beta - \gamma)\left(S_2 - \bar{S}\right) = \gamma\left(I_2 - \bar{I}\right) - D\left(\frac{\theta}{I_2} - 1\right). \tag{35b}$$

Addenda signs in (35a)–(35b) impose that $\bar{I} > I_2 > \theta$, which contradicts the initial assumption.

- $S_1 \leq \bar{S}$, $I_2 > \theta$. Then, sign of (35b) RHS implies that $S_2 > \bar{S} \geq S_1$, which, however, is in contrast with (35a).

Since in any case we find a contradiction, θ must belong to the interval (31). □

Remark 2. Note that when θ belongs to the interval (31), pseudo–equilibria are the unique possible attractors of model (1)–(3). Indeed, from (3), neither E_2 nor $E_2^{\bar{c}}$ can exist.

Theorem 3.8. *A pseudo–equilibrium of model (1)–(3) is locally asymptotically stable if, and only if,*

$$(d_1+d_2)\left[d_3(d_1+d_2+d_3)+\gamma D\frac{S_2^2}{S_1}+\beta S_1 d_2\right]+ \tag{36}$$
$$+(\beta^2-\gamma^2)S_2I_2(d_2+d_3)-\frac{D^2}{\theta}(\beta-\gamma)S_1I_2>0,$$

with

$$d_1=\beta S_1+D\frac{S_2}{S_1},\quad d_2=\gamma S_2+D\frac{S_1}{S_2},\quad d_3=\gamma I_2+D\frac{\theta}{I_2}. \tag{37}$$

Proof. From (32), the Jacobian matrix of system (5) at a pseudo–equilibrium reads

$$J=\begin{bmatrix} -d_1 & D & -\frac{D}{\theta}S_1 \\ D & -d_2 & -(\beta+\gamma)S_2 \\ 0 & (\beta-\gamma)I_2 & -d_3 \end{bmatrix},$$

with d_1, d_2 and d_3 given in (37). With simple algebraic calculations, we derive the characteristic polynomial of J (say, $P(\lambda)$):

$$P(\lambda)=l_0+l_1\lambda+l_2\lambda^2+\lambda^3,$$

where

$$\begin{aligned} l_0 =&(\beta^2-\gamma^2)S_2I_2d_1+\left(\gamma D\frac{S_2^2}{S_1}+\beta S_1d_2\right)d_3+\frac{D^2}{\theta}(\beta-\gamma)S_1I_2\\ l_1 =&(d_1+d_2)d_3+(\beta^2-\gamma^2)S_2I_2+\gamma D\frac{S_2^2}{S_1}+\beta S_1d_2\\ l_2 =&d_1+d_2+d_3. \end{aligned}$$

Being $l_i>0$, $\forall i=0,\dots,2$, the presence of positive real roots for $P(\lambda)$ is excluded in virtue of Descartes' rule of sign. According to Routh–Hurwitz theorem, also complex roots with positive real part are not admissible if, and only if, $l_1l_2-l_0>0$, which corresponds to (36). □

The analytical condition (36) provided in Theorem 3.8 depends in a complicated manner on unknown pseudo–equilibrium values as well as on crucial parameters, like β, γ, D, θ; hence, it is difficult to give easier sufficient conditions for its positivity. However, in the specific case the hosts are very infrequent dispersers (i.e. $D\to 0$), which corresponds to the scenario where culling leads to an increase of infected individuals in the uncontrolled patch, expression (36) is always verified. In this case, a pseudo–equilibrium of model (1)–(3) is locally asymptotically stable.

Since the analytical results provided in Theorems 3.7 and 3.8 are not exhaustive, we perform different sets of numerical simulations on a wide range of parameters combinations for θ and $\bar{c}$ (as in Fig. 4) and for different initial conditions of model (1) variables. For each pair of parameters θ and $\bar{c}$, we find a unique attractor regardless of the initial conditions chosen for the simulations. Specifically, we find that the only suitable attractors for model (1)–(3) are either stable equilibria or pseudo–equilibria (which represent points of the sliding set (4).

The bifurcation analysis of epidemic model (1)–(3) in the parameter space $[\theta,\bar{c}]$, derived from the continuation of stable equilibria and pseudo–equilibria found in the numerical simulations, is illustrated in Fig. 4. Fig. 4 shows that, for large values of culling threshold (θ), model (1)–(3) equilibrium is unique, namely a stable

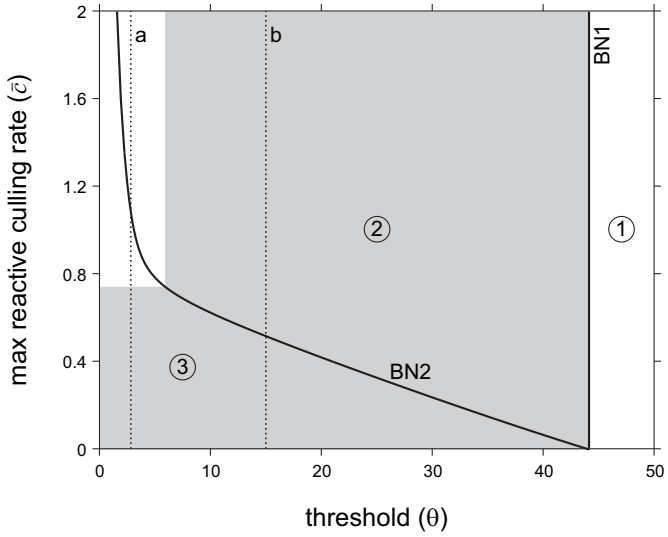

FIGURE 4. Bifurcation diagram of epidemic model (1)–(3) in the parameter space $[\theta, \bar{c}]$. The curves BN1 and BN2 represent boundary–node bifurcations. A stable equilibrium is the only attractor in regions 1 and 3. A pseudo–equilibrium is the only attractor in region 2. The shaded area represents the parameter combinations for which model (1)–(3) displays $I_2^{\theta,\bar{c}} > I_2^{0,0} = \bar{I}$. The relative variations of the number of infected individuals at model (1)–(3) steady–state with respect to the number of infected in the absence of control ($\delta I_j^{\theta,\bar{c}}$) as a function of parameter $\bar{c}$, corresponding to the dotted lines a and b, are illustrated in Figs. 5 and 6. Other parameters are: $r = 0.9$; $\mu = 0.2$; $K = 600$; $\mathcal{R}_0 = 10$; $\alpha = 0$, $D = 0.1r$.

equilibrium (independent from the values assumed by $\bar{c}$) corresponding to endemic equilibrium (14) as defined in continuous model (1) in the absence of control, namely E_2 (see region 1 in Fig. 4). By decreasing threshold θ, equilibrium E_2 found in region 1 undergoes a boundary–node bifurcation for $\theta = I_1^{0,0} = I_2^{0,0} = \bar{I}$ (line BN1 in Fig. 4), where $I_j^{\theta,\bar{c}}$ denotes the steady–state value of infected individuals in patches j for localized reactive control (3) with parameters θ, $\bar{c}$. By crossing BN1 and entering region 2 the original E_2 equilibrium disappears and a pseudo–equilibrium characterized by $I_1^{\theta,\bar{c}} = \theta$ appears (see region 2 in Fig. 4). Curve BN2 represents a boundary–node bifurcation: by crossing it and entering region 3, the pseudo–equilibrium characterized by $I_1^{\theta,\bar{c}} = \theta$ disappears and a stable equilibrium characterized by $I_1^{\theta,\bar{c}} > \theta$ appears. Boundary–node bifurcations BN1 and BN2 correspond to the vanishing of the vector fields $f_1^{(2)}$ and $f_2^{(2)}$, respectively, as defined in (4). The grey area in Fig. 4 represents the conditions in the parameter space $[\theta, \bar{c}]$ where $I_2^{\theta,\bar{c}} > I_2^{0,0} = \bar{I}$, i.e., where localized reactive culling is ineffective in reducing the infection burden in both areas. Specifically, Fig. 4 shows that, in the case of low levels of culling threshold θ, sufficiently high efforts of culling, $\bar{c}$, are able to reduce the infection burden in both areas, as in the case of localized proactive

culling (see solid line in Fig. 3). On the other hand, in the case of intermediate values of θ, localized reactive culling is ineffective in reducing the infection burden in both areas regardless of the culling effort applied in disease control. These findings are highlighted in Figs. 5 and 6, where the effects of localized reactive control on the relative variation of the number of infected individuals in patches 1 (panels A) and 2 (panels B) at model (1)–(3) steady–state with respect to the number of infected in the absence of control ($\delta I_j^{\theta,\bar{c}} = (I_j^{\theta,\bar{c}} - \bar{I})/\bar{I}$, with $j = 1, 2$) are shown for two different levels of culling threshold ($\theta = 2.5$ in Fig. 5, $\theta = 15$ in Fig. 6).

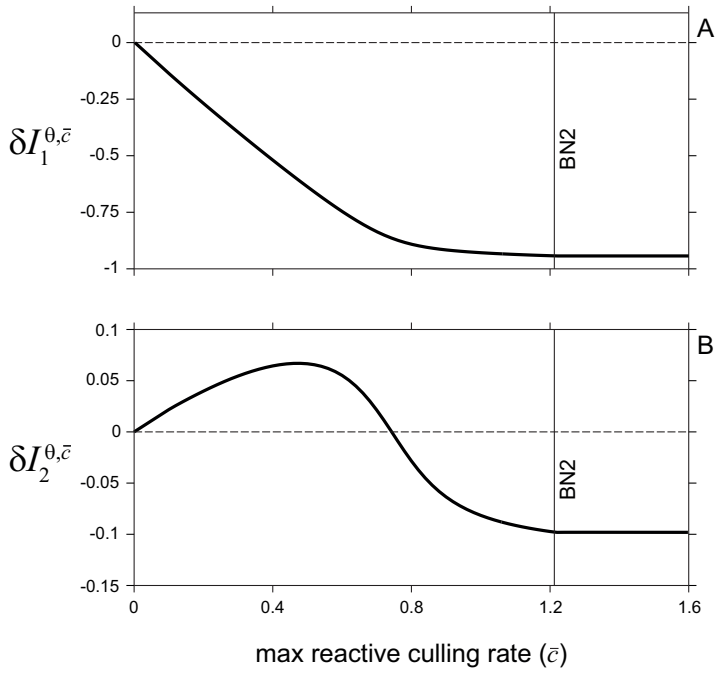

FIGURE 5. Relative variation of the number of infected individuals in patches 1 (panel A) and 2 (panel B) at model (1)–(3) steady–state with respect to the number of infected in the absence of control ($\delta I_j^{\theta,\bar{c}}$, with $j = 1, 2$) as a function of parameter $\bar{c}$. BN2 represents a boundary–node bifurcation point as in Fig. 4. The dashed line represents the condition $I_j^{\theta,\bar{c}} = \bar{I}$. Parameter $\theta = 2.5$, unspecified parameters as in Fig. 4.

4. **Discussion.** In this paper, we analyze the effect of localized proactive and reactive culling on the disease dynamics in a metapopulation model with two patches (one with control and the other one without control). Proactive culling is described through a classical ODE continuous system, while reactive culling is described through a discontinuous piecewise–smooth system where the control activities are implemented when the number of infected individuals exceeds a given threshold. Models implementing sliding control have been already developed in recent years for different infections, such as West Nile Virus [48], avian influenza [17, 16], and SARS [47]. Here, we find that, localized culling implemented in one of the patches

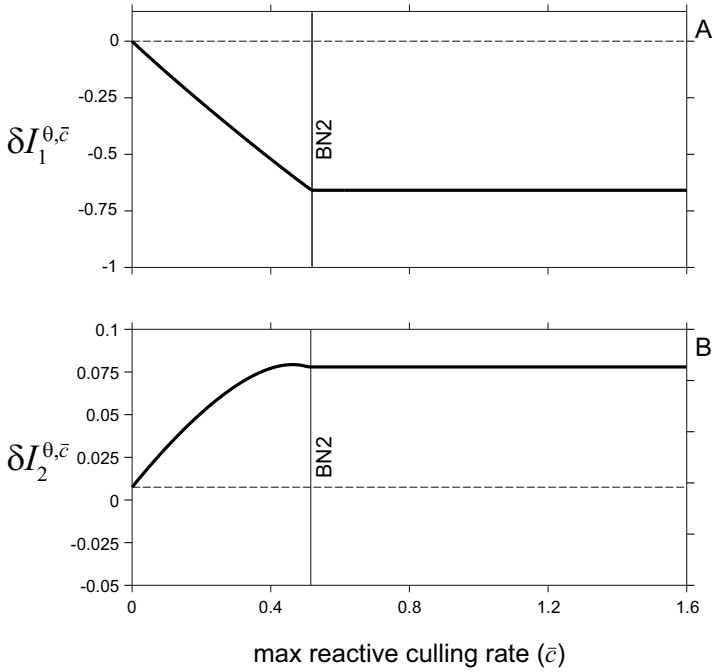

FIGURE 6. Relative variation of the number of infected individuals in patches 1 (panel A) and 2 (panel B) at model (1)–(3) steady–state with respect to the number of infected in the absence of control ($\delta I_j^{\theta,\bar{c}}$, with $j = 1, 2$) as a function of parameter $\bar{c}$. BN2 represents a boundary–node bifurcation point as in Fig. 4. The dashed line represents the condition $I_j^{\theta,\bar{c}} = \bar{I}$. Parameter $\theta = 15$, unspecified parameters as in Fig. 4.

may lead to an unexpected increase in the number of infected individuals in the other patch. In the case of continuous model (1)–(2), we provide the necessary conditions for this counter–intuitive outcome to occur (see Theorem 3.6). In details, the equilibrium value of infected individuals $\hat{I}_2$ in presence of proactive culling can increase only if $2D < r$ (hosts are very infrequent dispersers) and $\mathcal{R}_0 > 2$, namely if the basic reproduction number of the corresponding uncontrolled model is at least twice the endemicity threshold. In addition, we numerically find that the number of infected individuals in the uncontrolled patch eventually peaks for intermediate values of culling and then decreases only for high level of culling effort (see Fig. 3). On the other hand, in sliding model (1)–(3), we numerically find that, for intermediate levels of disease detection, localized reactive culling increases the infection burden in the uncontrolled patch regardless of the culling effort applied in the disease control (see Figs. 4 and 6B).

The biological explanation for this unexpected effect relies on the remark that, when the dispersal rate (D) is low, the introduction of culling induces an increase in the number of susceptible individuals in both the controlled and uncontrolled patches (see Theorem 3.6 and Proposition 1). This leads to a flush of new susceptibles entering the uncontrolled patch, then providing a bust to the infection transmission. We

have proved the generality of this result by showing that it does not depend on the specific assumptions made in model (1), but it holds also relaxing the hypotheses of disease–induced host sterility and density–dependent mortality in the infection model (see Remark 1).
The epidemiological and economic conditions leading to the ineffectiveness of disease control through culling have also been investigated in optimal control frameworks. Bolzoni *et al.* [8] showed that reactive culling implemented around the peak of infection represents an optimal control strategy only when the basic reproduction number of the infection is low and the costs of control are high.
In conclusion, this paper shows that also in the absence of the density–dependent compensatory effects – which were previously associated to disease control failure –, localized culling may represent an ineffective strategy in limiting infectious diseases in wildlife.

Appendix A. **The control reproduction number $\mathcal{R}_C$.** Following the procedure and the notations in [22, 44], we prove that the control reproduction number of model (1)–(2), $\mathcal{R}_C$, is given by (20).

Let us consider the RHS of equations (1b) and (1d), with $c = \bar{c}$, and distinguish the new infections appearance from the other rates of transfer, by defining the vectors

$$\mathcal{F} = \begin{bmatrix} \beta S_1 I_1 \\ \beta S_2 I_2 \end{bmatrix} \quad \text{and} \quad \mathcal{V} = \begin{bmatrix} (\mu+\alpha+\bar{c}+\gamma N_1)I_1 + DI_1 - DI_2 \\ (\mu+\alpha+\gamma N_2)I_2 + DI_2 - DI_1 \end{bmatrix}.$$

The Jacobian matrices of $\mathcal{F}$ and $\mathcal{V}$ evaluated at model (1)–(2) disease–free equilibrium $E_1^{\bar{c}} = [\hat{K}_1, 0, \hat{K}_2, 0]$ read, respectively,

$$F = \begin{bmatrix} \beta\hat{K}_1 & 0 \\ 0 & \beta\hat{K}_2 \end{bmatrix} \quad \text{and} \quad V = \begin{bmatrix} \mu+\alpha+\bar{c}+\gamma\hat{K}_1+D & -D \\ -D & \mu+\alpha+\gamma\hat{K}_2+D \end{bmatrix}.$$

As proved in [22, 44], the control reproduction number is given by the spectral radius of the *next generation* matrix FV^{-1}. Simple algebra yields

$$(FV^{-1})_{11} = \frac{\beta\hat{K}_1\left(\mu+\alpha+\gamma\hat{K}_2+D\right)}{\left(\mu+\alpha+\bar{c}+\gamma\hat{K}_1+D\right)\left(\mu+\alpha+\gamma\hat{K}_2+D\right)-D^2}$$

$$(FV^{-1})_{12} = \frac{\beta\hat{K}_1 D}{\left(\mu+\alpha+\bar{c}+\gamma\hat{K}_1+D\right)\left(\mu+\alpha+\gamma\hat{K}_2+D\right)-D^2}$$

$$(FV^{-1})_{21} = \frac{\beta\hat{K}_2 D}{\left(\mu+\alpha+\bar{c}+\gamma\hat{K}_1+D\right)\left(\mu+\alpha+\gamma\hat{K}_2+D\right)-D^2}$$

$$(FV^{-1})_{22} = \frac{\beta\hat{K}_2\left(\mu+\alpha+\bar{c}+\gamma\hat{K}_1+D\right)}{\left(\mu+\alpha+\bar{c}+\gamma\hat{K}_1+D\right)\left(\mu+\alpha+\gamma\hat{K}_2+D\right)-D^2},$$

and, being the eigenvalues $\lambda_\pm$ of FV^{-1} given by

$$\lambda_\pm = \frac{1}{2}\beta\frac{\hat{K}_1(\mu+\alpha+D)+\hat{K}_2(\mu+\alpha+\bar{c}+D)+2\gamma\hat{K}_1\hat{K}_2 \pm \sqrt{\Delta_C}}{\left(\mu+\alpha+\bar{c}+\gamma\hat{K}_1+D\right)\left(\mu+\alpha+\gamma\hat{K}_2+D\right)-D^2},$$

with Δ_C as in (21), we get (20).

Appendix B. **Ineffectiveness of proactive culling by relaxing some hypotheses.** Let us consider the following metapopulation epidemic model

$$\dot{S}_1 = \nu N_1 - \beta S_1 I_1 - (\mu + c) S_1 - D S_1 + D S_2 \tag{38a}$$

$$\dot{I}_1 = \beta S_1 I_1 - (\mu + \alpha + c) I_1 - D I_1 + D I_2 \tag{38b}$$

$$\dot{S}_2 = \nu N_2 - \beta S_2 I_2 - \mu S_2 - D S_2 + D S_1 \tag{38c}$$

$$\dot{I}_2 = \beta S_2 I_2 - (\mu + \alpha) I_2 - D I_2 + D I_1, \tag{38d}$$

that differs from model (1) in the absence of both pathogen–induced sterility (also infected individuals reproduce) and density–dependent mortality for susceptibles ($\gamma = 0$). Remember that we called $r = \nu - \mu$ the intrinsic growth rate.
Firstly, one can easily check that, in the absence of control ($c = 0$), an endemic equilibrium (say, E_2) exists only if $\alpha > r$ and has components equal in pairs [23]: $E_2 = [\bar{S}, \bar{I}, \bar{S}, \bar{I}]$, where

$$\bar{S} = \frac{\mu + \alpha}{\beta} \tag{39a}$$

$$\bar{I} = \frac{r(\mu + \alpha)}{\beta(\alpha - r)}. \tag{39b}$$

For E_2 stability properties, see [23].
Then, let us denote with $E_2^{\bar{c}} = [\hat{S}_1(\bar{c}), \hat{I}_1(\bar{c}), \hat{S}_2(\bar{c}), \hat{I}_2(\bar{c})]$ the generic endemic equilibrium of model (38) with $c = \bar{c}$. By differentiating with respect to $\bar{c}$ the RHS side of equations (38) at $E_2^{\bar{c}}$, we obtain

$$\begin{aligned}\beta \hat{I}_1'(\bar{c}) =& -1 + \frac{\nu}{\hat{S}_1^2(\bar{c})}[\hat{I}_1'(\bar{c})\hat{S}_1(\bar{c}) - \hat{S}_1'(\bar{c})\hat{I}_1(\bar{c})] \\ &+ \frac{D}{\hat{S}_1^2(\bar{c})}[\hat{S}_2'(\bar{c})\hat{S}_1(\bar{c}) - \hat{S}_1'(\bar{c})\hat{S}_2(\bar{c})]\end{aligned} \tag{40a}$$

$$\beta \hat{S}_1'(\bar{c}) = 1 - \frac{D}{\hat{I}_1^2(\bar{c})}[\hat{I}_2'(\bar{c})\hat{I}_1(\bar{c}) - \hat{I}_1'(\bar{c})\hat{I}_2(\bar{c})] \tag{40b}$$

$$\begin{aligned}\beta \hat{I}_2'(\bar{c}) =& \frac{\nu}{\hat{S}_2^2(\bar{c})}[\hat{I}_2'(\bar{c})\hat{S}_2(\bar{c}) - \hat{S}_2'(\bar{c})\hat{I}_2(\bar{c})] \\ &+ \frac{D}{\hat{S}_2^2(\bar{c})}[\hat{S}_1'(\bar{c})\hat{S}_2(\bar{c}) - \hat{S}_2'(\bar{c})\hat{S}_1(\bar{c})]\end{aligned} \tag{40c}$$

$$\beta \hat{S}_2'(\bar{c}) = -\frac{D}{\hat{I}_2^2(\bar{c})}[\hat{I}_1'(\bar{c})\hat{I}_2(\bar{c}) - \hat{I}_2'(\bar{c})\hat{I}_1(\bar{c})]. \tag{40d}$$

Of course, when $\bar{c} = 0$, $\hat{S}_j(0) = \bar{S}$ and $\hat{I}_j(0) = \bar{I}$, as given in (39). Then – by substituting the expressions for $\hat{S}_1'(0)$ and $\hat{S}_2'(0)$ (derived in (40b) and (40d), respectively) as functions of $\hat{I}_1'(0)$ and $\hat{I}_2'(0)$ –, we can re–write (40a) and (40c) as follows:

$$A(\bar{S}, \bar{I})\hat{I}_1'(0) = -\beta - \frac{D}{\bar{S}} - \frac{\nu \bar{I}}{\bar{S}^2} + B(\bar{S}, \bar{I})\hat{I}_2'(0) \tag{41a}$$

$$A(\bar{S}, \bar{I})\hat{I}_2'(0) = \frac{D}{\bar{S}} + B(\bar{S}, \bar{I})\hat{I}_1'(0), \tag{41b}$$

where

$$A(\bar{S}, \bar{I}) = \beta\left(\beta - \frac{\nu}{\bar{S}}\right) + B(\bar{S}, \bar{I}),$$

and

$$B(\bar{S},\bar{I}) = \frac{D\nu}{\bar{S}^2} + 2\frac{D^2}{\bar{S}\bar{I}}.$$

By substituting (41a) in (41b) and rearranging, we find the equation

$$\frac{A^2 - B^2}{A}\hat{I}_2'(0) = -\left(\beta + \frac{\nu\bar{I}}{\bar{S}^2}\right)\frac{B}{A} + \left(1 - \frac{B}{A}\right)\frac{D}{\bar{S}}. \tag{42}$$

Since $A(\bar{S},\bar{I}) > B(\bar{S},\bar{I})$, condition $\hat{I}_2'(0) > 0$ is fulfilled if and only if the RHS of (42) is positive. With simple algebraic manipulations – and remembering equalities (39) – then yields to

$$(\alpha - r)\left(1 - \frac{2D}{r}\right) - \nu - \frac{\nu}{\mu + \alpha}\left(\frac{r\nu}{\alpha - r} + 2D\right) > 0.$$

Acknowledgments. The authors wish to acknowledge the anonymous referees, whose several suggestions helped us to significantly improve the quality and the readability of the paper. This work was performed in the frame of the activities sponsored by the National Group of Mathematical Physics (GNFM–INdAM) and by the University of Parma (Italy). Support by the Italian Ministry of Education, University and Research (MIUR), PRIN research grant n. 2017YBKNCE, is also gratefully acknowledged.

REFERENCES

[1] R. M. Anderson and R. M. May, Population biology of infectious diseases: Part I, *Nature*, **280** (1979), 361–367.

[2] R. M. Anderson, H. C. Jackson, R. M. May and A. M. Smith, Population dynamics of fox rabies in Europe, *Nature*, **289** (1981), 765.

[3] J. Bielby, C. A. Donnelly, L. C. Pope, T. Burke and R. Woodroffe, Badger responses to small–scale culling may compromise targeted control of bovine tuberculosis, *Proceedings of the National Academy of Sciences*, **111** (2014), 9193–9198, URL http://www.pnas.org/content/111/25/9193.

[4] J. Bielby, F. Vial, R. Woodroffe and C. A. Donnelly, Localised badger culling increases risk of herd breakdown on nearby, not focal, land, *PLoS ONE*, **11** (2016), 1–9, URL https://doi.org/10.1371/journal.pone.0164618.

[5] L. Bolzoni and G. A. De Leo, Unexpected consequences of culling on the eradication of wildlife diseases: the role of virulence evolution, *American Naturalist*, **181** (2013), 301–313.

[6] L. Bolzoni, G. A. De Leo, M. Gatto and A. P. Dobson, Body-size scaling in an SEI model of wildlife diseases, *Theoretical Population Biology*, **73** (2008), 374–382.

[7] L. Bolzoni, L. Real and G. De Leo, Transmission heterogeneity and control strategies for infectious disease emergence, *PLoS ONE*, **2** (2007), e747.

[8] L. Bolzoni, V. Tessoni, M. Groppi and G. A. De Leo, React or wait: which optimal culling strategy to control infectious diseases in wildlife, *Journal of Mathematical Biology*, **69** (2014), 1001–1025.

[9] L. Bolzoni, E. Bonacini, R. Della Marca and M. Groppi, Optimal control of epidemic size and duration with limited resources, *Mathematical Biosciences*, **315** (2019), 108232, URL http://www.sciencedirect.com/science/article/pii/S002555641830511X.

[10] L. Bolzoni, E. Bonacini, C. Soresina and M. Groppi, Time–optimal control strategies in SIR epidemic models, *Mathematical Biosciences*, **292** (2017), 86–96.

[11] M. H. Bond, Host life-history strategy explains pathogen-induced sterility, *American Naturalist*, **168** (2006), 281–293.

[12] M. S. Boyce, A. R. E. Sinclair and G. C. White, Seasonal compensation of predation and harvesting, *Oikos*, **87** (1999), 419–426, URL http://www.jstor.org/stable/3546808.

[13] S. P. Carter, R. J. Delahay, G. C. Smith, D. W. Macdonald, P. Riordan, T. R. Etherington, E. R. Pimley, N. J. Walker and C. L. Cheeseman, Culling–induced social perturbation in Eurasian badgers *Meles meles* and the management of TB in cattle: an analysis of a critical problem in applied ecology, *Proceedings of the Royal Society of London B: Biological Sciences*, **274** (2007), 2769–2777, URL http://rspb.royalsocietypublishing.org/content/274/1626/2769.

[14] R. Casagrandi and M. Gatto, A persistence criterion for metapopulations, *Theoretical Population Biology*, **61** (2002), 115 – 125, URL http://www.sciencedirect.com/science/article/pii/S0040580901915588.

[15] M. Choisy and P. Rohani, Harvesting can increase severity of wildlife disease epidemics, *Proceedings of the Royal Society B*, **273** (2006), 2025–2034.

[16] N. S. Chong, B. Dionne and R. J. Smith, An avian-only Filippov model incorporating culling of both susceptible and infected birds in combating avian influenza, *Journal of Mathematical Biology*, **73** (2016), 751784.

[17] N. S. Chong and R. J. Smith, Modeling avian influenza using Filippov systems to determine culling of infected birds and quarantine, *Nonlinear Analysis: Real World Applications*, **24** (2015), 196218.

[18] S. Cleaveland, K. Laurenson and T. Mlengeya, Impacts of wildlife infections on human and livestock health with special reference to Tanzania: Implications for protected area management, in *Conservation and Development Interventions at the Wildlife/Livestock Interface: Implications for Wildlife, Livestock and Human Health* (eds. S. Osofsky, S. Cleaveland, W. Karesh, M. Kock, P. Nyhus, L. Starr and A. Yang), IUCN, Gland, 2005, 147–151.

[19] M. J. Coyne, G. Smith and F. E. McAllister, Mathematic model for the population biology of rabies in raccoons in the mid–Atlantic states., *American Journal of Veterinary Research*, **50** (1989), 2148–2154.

[20] F. Dercole, A. Gragnani, Y. A. Kuznetsov and S. Rinaldi, Numerical sliding bifurcation analysis: an application to a relay control system, *IEEE Transactions on Circuits and Systems I: Fundamental Theory and Applications*, **50** (2003), 1058–1063.

[21] F. Dercole and Y. A. Kuznetsov, Slidecont: An Auto97 driver for sliding bifurcation analysis, *ACM Transactions on Mathematical Software*, **31** (2005), 95–119.

[22] O. Diekmann, J. A. P. Heesterbeek and J. A. J. Metz, On the definition and the computation of the basic reproduction ratio R_0 in models for infectious diseases in heterogeneous populations, *Journal of Mathematical Biology*, **28** (1990), 365–382, URL https://doi.org/10.1007/BF00178324.

[23] O. Diekmann and M. Kretzschmar, Patterns in the effects of infectious diseases on population growth, *Journal of Mathematical Biology*, **29** (1991), 539–570.

[24] E. J. Doedel, A. R. Champneys, T. F. Fairgrieve, Y. A. Kuznetsov, B. Sandstede and X. Wang, *Auto97: Continuation and bifurcation software for ordinary differential equaitions (with HomCont)*, Computer Science, Concordia University, Montreal, Canada, 1997.

[25] K. Dong-Hyun, Structural factors of the Middle East respiratory syndrome coronavirus outbreak as a public health crisis in Korea and future response strategies, *Journal of Preventive Medicine and Public Health*, **48** (2015), 265–270.

[26] C. A. Donnelly, R. Woodroffe, D. R. Cox, F. J. Bourne, C. Cheeseman, R. S. Clifton-Hadley, G. Wei, G. Gettinby, P. Gilks, H. Jenkins, W. T. Johnston, A. M. Le Fevre, J. P. McInerney and W. I. Morrison, Positive and negative effects of widespread badger culling on tuberculosis in cattle, *Nature*, **439** (2006), 843.

[27] C. A. Donnelly, R. Woodroffe, D. R. Cox, J. Bourne, G. Gettinby, A. M. Le Fevre, J. P. McInerney and W. I. Morrison, Impact of localized badger culling on tuberculosis incidence in British cattle, *Nature*, **426** (2003), 834.

[28] A. F. Filippov, *Differential equations with discontinuous righthand sides*, Kluwer Acad. Publ., Dordrecht, 1988.

[29] L. G. Frank and R. Woddroffe, Behaviour of carnivores in exploited and controlled populations, in *Carnivore Conservation* (eds. J. Gittleman, S. Funk, D. Macdonald and R. Wayne), Cambridge University Press, Cambridge, 2001, 419–442.

[30] P. Glendinning and M. R. Jeffrey, Grazing-sliding bifurcations, border collision maps and the curse of dimensionality for piecewise smooth bifurcation theory, *Nonlinearity*, **28** (2015), 263.

[31] S. J. Hogan, M. E. Homer, M. R. Jeffrey and R. Szalai, Piecewise smooth dynamical systems theory: the case of the missing boundary equilibrium bifurcations, *Journal of Nonlinear Science*, **26** (2016), 1161–1173.

[32] R. A. Horn and C. R. Johnson, *Matrix Analysis*, Cambridge University Press, New York, USA, 1986.
[33] K. E. Jones, N. G. Patel, M. A. Levy, A. Storeygard, D. Balk, J. L. Gittleman and P. Daszak, Global trends in emerging infectious diseases, *Nature*, **451** (2008), 990.
[34] A. J. Kucharski, A. Camacho, S. Flasche, R. E. Glover, W. J. Edmunds and S. Funk, Measuring the impact of Ebola control measures in Sierra Leone, *Proceedings of the National Academy of Sciences*, **112** (2015), 14366–14371, URL http://www.pnas.org/content/112/46/14366.
[35] Y. A. Kuznetsov, S. Rinaldi and A. Gragnani, One-parameter bifurcations in planar Filippov systems, *International Journal of Bifurcation and Chaos*, **8** (2003), 2157–2188.
[36] S. Lachish, H. Mccallum, D. Mann, C. E. Pukk and M. E. Jones, Evaluation of selective culling of infected individuals to control Tasmanian devil facial tumor disease, *Conservation Biology*, **24** (2010), 841–851, URL https://onlinelibrary.wiley.com/doi/abs/10.1111/j.1523-1739.2009.01429.x.
[37] M. K. Morters, O. Restif, K. Hampson, S. Cleaveland, J. L. N. Wood and A. J. K. Conlan, Evidence–based control of canine rabies: a critical review of population density reduction, *Journal of Animal Ecology*, **82** (2013), 6–14, URL https://besjournals.onlinelibrary.wiley.com/doi/abs/10.1111/j.1365-2656.2012.02033.x.
[38] P. T. Piiroinen and Y. A. Kuznetsov, An event-driven method to simulate Filippov systems with accurate computing of sliding motions, *ACM Transactions on Mathematical Software*, **34** (2008), 13.
[39] L. C. Pope, R. K. Butlin, G. J. Wilson, R. Woodroffe, K. Erven, C. M. Conyers, T. Franklin, R. J. Delahay, C. L. Cheeseman and T. Burke, Genetic evidence that culling increases badger movement: implications for the spread of bovine tuberculosis, *Molecular Ecology*, **16** (2007), 4919–4929, URL https://onlinelibrary.wiley.com/doi/abs/10.1111/j.1365-294X.2007.03553.x.
[40] M. J. Smith, A. White, J. A. Sherratt, S. Telfer, M. Begon and X. Lambin, Disease effects on reproduction can cause population cycles in seasonal environments, *Journal of Animal Ecology*, **77** (2008), 378–389.
[41] S. H. Strogatz, *Nonlinear Dynamics and Chaos*, Perseus Books Publishing, Reading, Massachussetts, 1994.
[42] M. I. Tosa, E. M. Schauber and C. K. Nielsen, Localized removal affects white–tailed deer space use and contacts, *The Journal of Wildlife Management*, **81** (2017), 26–37, URL https://wildlife.onlinelibrary.wiley.com/doi/abs/10.1002/jwmg.21176.
[43] F. A. M. Tuyttens, D. W. Macdonald, L. M. Rogers, C. L. Cheeseman and A. W. Roddam, Comparative study on the consequences of culling badgers (*Meles meles*) on biometrics, population dynamics and movement, *Journal of Animal Ecology*, **69** (2000), 567–580, URL https://besjournals.onlinelibrary.wiley.com/doi/abs/10.1046/j.1365-2656.2000.00419.x.
[44] P. Van den Driessche and J. Watmough, Reproduction numbers and sub–threshold endemic equilibria for compartmental models of disease transmission, *Mathematical Biosciences*, **180** (2002), 29–48.
[45] F. Vial and C. A. Donnelly, Localized reactive badger culling increases risk of bovine tuberculosis in nearby cattle herds, *Biology Letters*, **8** (2012), 50–53.
[46] R. Woodroffe, S. Cleaveland, O. Courtenay, M. K. Laurenson and M. Artois, Infectious disease in the management and conservation of wild canids, in *The Biology and Conservation of Wild Canids* (eds. D. Macdonald and C. Sillero-Zubiri), Oxford University Press, Oxford, 2004, 124–142.
[47] Y. Xiao, X. Xu and S. Tang, Sliding mode control of outbreaks of emerging infectious diseases, *Bulletin of Mathematical Biology*, **74** (2012), 2403–2422.
[48] Y. Xiao, X. Xu and S. Tang, A threshold policy to interrupt transmission of West Nile Virus to birds, *Applied Mathematical Modelling*, **40** (2016), 8794–8809.

Received xxxx 20xx; revised xxxx 20xx.

E-mail address: luca.bolzoni@izsler.it
E-mail address: rossella.dellamarca@unipr.it
E-mail address: maria.groppi@unipr.it
E-mail address: alessandra.gragnani@polimi.it